Available online at www.sciencedirect.com
SCIENCE DIRECT
Surface & Coatings Technology 200 (2005) 1751 – 1754
SURFACE & COATINGS TECHNOLOGY
www.elsevier.com/locate/surfcoat

The effect of CeO_2 abrasive size on dishing and step height reduction of silicon oxide film in STI–CMP

D.S. Lim [a,*], J.W. Ahn [a], H.S. Park [b], J.H. Shin [b]

[a] Department of Material Science and Engineering, Korea University, Anam-Dong 5-1, Sungbuk-Ku, Seoul, 136-701, South Korea
[b] Memory Research and Development Division, Hynix Semiconductor Inc., San 136-1, Ami-ri, Bubal-eub, Ichon-si, Kyoungki-do, 467-701, South Korea

Available online 30 September 2005

Abstract

The effect of the CeO_2 abrasive size during chemical mechanical polishing (CMP) of shallow trench isolation (STI) structures was investigated, in order to minimize the amount of oxide dishing and to improve the planarization efficiency. Three slurry samples were prepared based on a 1.0 wt.% abrasive concentration with different sizes of ceria particles. The step height and dishing reduction were investigated as a function of the polishing time with pattern wafers in prepared slurries. The reduction in thickness as a function of the polishing time varied between the different slurries. The dependence of the step height reduction of the patterned wafer on the polishing time showed non-linear behavior in all of the tested slurries. The amount of dishing also varied with the type of slurry. The changes in the cross-sectional profiles of the oxide as a function of the polishing time were analyzed, in order to establish a dishing and step height reduction model depending on the abrasive size. The step height variation and dishing were varied with the size of the abrasive. The observed results were explained by the contribution of inactive particles, which depended on relative size of the abrasives and the height of the remaining oxide layer.

Keywords: Silicon oxide; Chemical mechanical polishing; Shallow trench isolation; Dishing; Oxide step height

1. Introduction

Shallow trench isolation (STI) has emerged as the primary technique for advanced ultra large-scale integration (ULSI) technologies [1,2]. STI improves the isolation and increases the device packing density. However, STI requires a planarization process. Several issues associated with chemical mechanical planarization (CMP) need to be solved, since the requirements for STI planarization are much more severe than those for inter-layer dielectric (ILD) planarization [3]. STI structures consist of nitride and oxide deposition as shown in Fig. 1. Oxide remnants above the silicon nitride, erosion and trench oxide dishing during CMP process are frequently observed during STI planarization as shown in Fig. 1b. These defects are undesirable, since they degrade the quality of the isolation and damage the edge of the silicon active area [4–6].

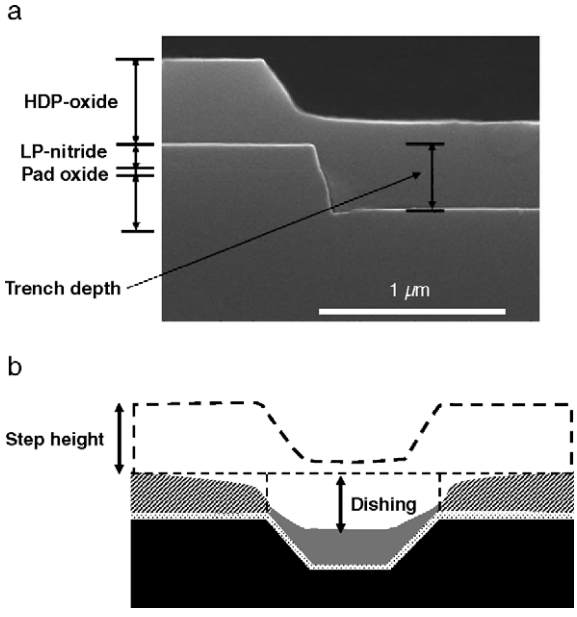

Fig. 1. SEM micrograph of cross-section al view showing (a) trench oxide filling and (b) definition of step height and dishing in STI structures.

* Corresponding author. Tel.: +82 2 3290 3272; fax: +82 2 929 5344.
E-mail address: dslim@korea.ac.kr (D.S. Lim).

0257-8972/$ - see front matter © 2005 Elsevier B.V. All rights reserved.
doi:10.1016/j.surfcoat.2005.08.047

Table 1
Comparison of slurries used in this experiment

Items	Ceria-based slurry		
Types of slurry	Slurry A	Slurry B	Slurry C
Primary particle size (nm)	45	175	225
Slurry mean size	179	312	348
Solid loading	1 wt.%		
Base solution	D.I. water		
pH	6.7		

Different approaches have been attempted to reduce the amount of dishing and erosion. The effect of the surface conditions and the hardness of the polishing pad and on the planarization has previously been studied [7–9]. Zhao and Shi also showed that low down-force polishing provides better planarization than high down-force STI–CMP [10]. The use of high selectivity slurries such as ceria-based slurry that improve the ability to halt the polishing at the nitride stop layer and reduce the amount of dishing was also reported [11–13]. Dishing and the generation of defects have remained an ongoing issue, however, despite the significant improvements in trench dishing that were achieved recently through the use of high selectivity slurries. To improve the planarization of the STI process, it is necessary to understand in detail the nature of the contact between the abrasive and the oxide layer. However, few studies have been conducted in order investigate the effect of the abrasive size on the variation in the step height. In this study, the effect of abrasive size on the variation in the oxide step height and the amount of dishing was examined, in order to provide guidelines for the achievement of good planarization performance for STI–CMP.

2. Experimental procedure

Fig. 1 shows the typical SEM images of the STI structure. This pattern is prepared as follows. The isolation mask is prepared by depositing a 129 nm thick LPCVD (low pressure chemical vapor deposited) nitride film on a 10 nm thick thermal pad. Following the photolithographic definition of the active area, the nitride/oxide stack is etched and 372 nm trenches are subsequently etched into the silicon substrate. After cleaning, a 10 nm sidewall oxidation step is performed. Next, the trenches are refilled using 457 nm HDP (high density plasma)-CVD oxide. Specimens with dimensions of 30×30 mm were diced from the 200 mm isolation pattern wafer. Each specimen contained a series of line patterns, which consisted of trenches with a width of 10 μm and a patterned width of 10 μm. CMP was carried out by means of a rotary type CMP machine (LPG-15AF, Lapmaster SFT Corp., Japan) using a polyurethane stack pad (IC1000/SUBA IV, Rodel). Three types of ceria-based slurry were used, in order to study the variation in the step height with the abrasive size. The slurries were prepared by using three different kinds of ceria abrasives as shown in Table 1. The abrasives were dispersed in deionized water. Commercial dispersant and anionic surfactant were added. The solid loading of the abrasives and organic slurry pH were fixed to 1 wt.% and 6.7, respectively. The polishing speeds of both the table and the head were maintained at 40

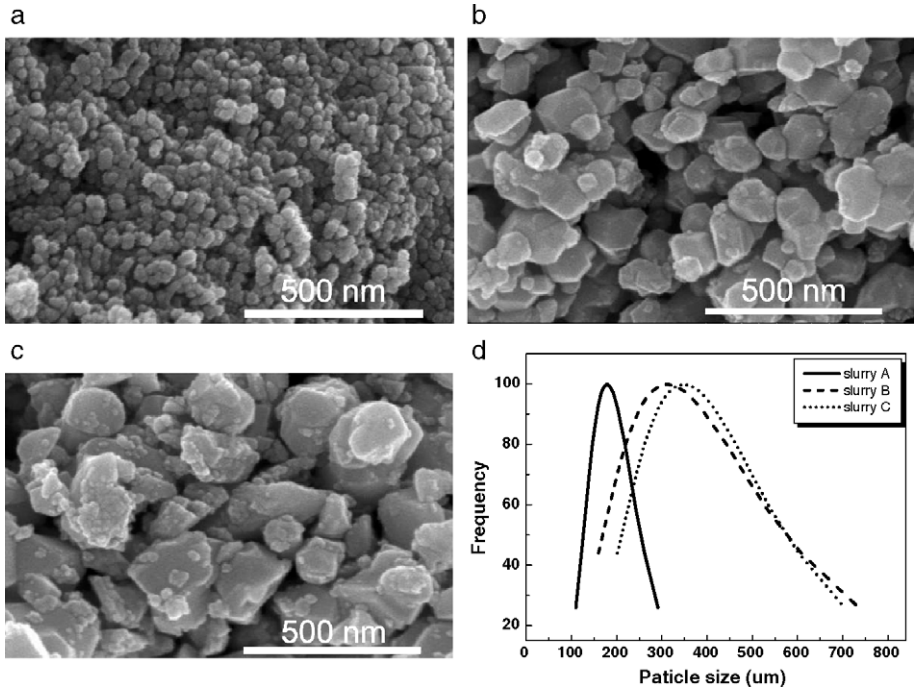

Fig. 2. SEM micrographs of ceria abrasives in (a) slurry A, (b) slurry B and (c) slurry C and (d) particle size distribution.

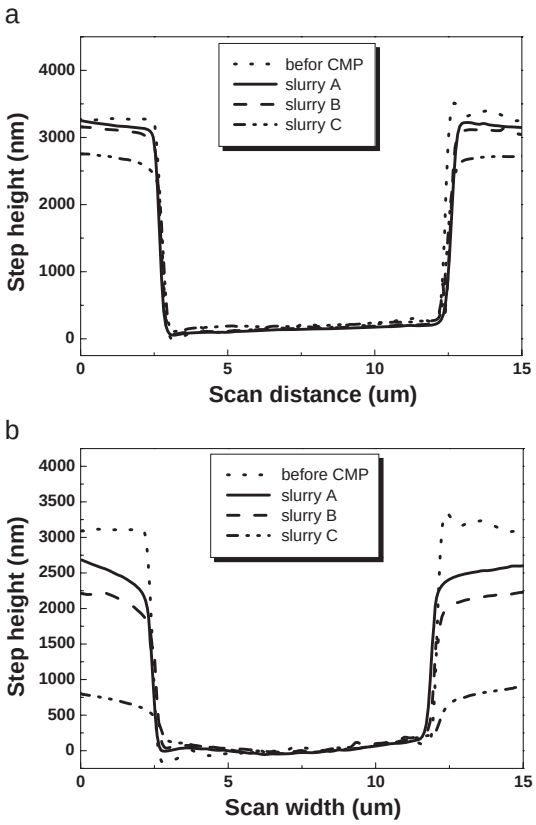

Fig. 3. Variation of oxide profiles with slurries A, B, and C after polishing for (a) 20 s, and (b) 60 s. Surface profiles were measured by atomic force profilometer.

rpm. The applied down pressure was set to approximately 27,580 N/m^2. The slurry feed rate was 50 cm^3/mm. Pad conditioning was performed for 30 s prior to each experiment using a diamond impregnated disk. The polished samples were cleaned with alcohol, acetone and DI water prior to the thickness and roughness measurements. The variation in the step height was measured by means of a surface profilometer (alpha-step 500, Tencor). The detailed

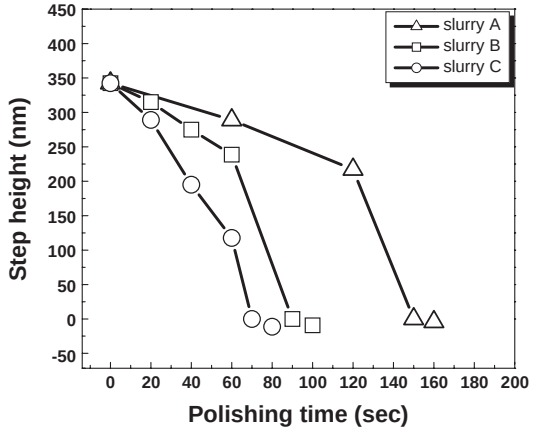

Fig. 4. Variation of step height as a function of polishing time with different types of slurries.

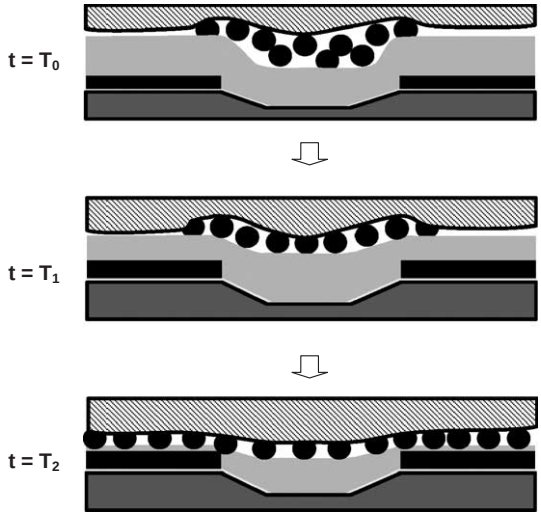

Fig. 5. Schematic diagrams showing time dependent nature of trapped inactive particles due to variation of the step height.

edge variation and roughness were examined by atomic force microscopy. The abrasive particles and polished samples were examined with FESEM. The size distributions of the abrasive in the slurries were measured by means of a particle size analyzer (Zetaplus, Brookhaven).

3. Results and discussion

Fig. 2 shows the three types of ceria particles used in this study. The average particle sizes determined in the SEM examination were 45 nm, 175 nm and 225 nm for slurries A, B and C, respectively. The ceria particles in slurry A were roughly spherical in shape. The results of the particle size analysis showed that the average size and particle distribution varied depending on the types of slurry. The CMP process removes the local steps and produces local planarity, as shown in Fig. 3. Fig. 4 shows the variation in the oxide step height with the type of slurry as a function of the polishing time. The step height decreases slowly at the

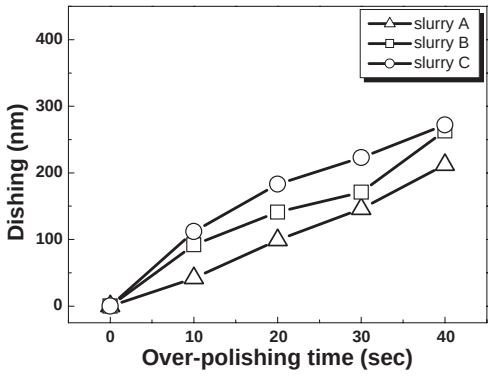

Fig. 6. Variation of dishing as a function of over-polishing time with three different slurries.

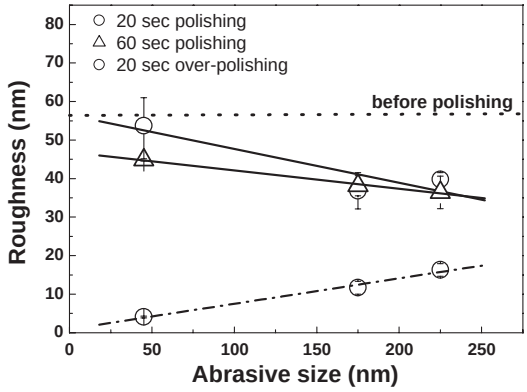

Fig. 7. Variation of dishing as a function of over-polishing time with three different slurries.

beginning of the polishing process and then more rapidly as polishing progresses for all three slurries. The initial removal rate of the oxide film increases with increasing particle size in the slurry. The transition from a slow to a rapid removal rate was unexpected, since the contact pressure between the pad and the wafer would be expected to decrease as polishing progresses. This unique characteristic can be explained as follows. Fig. 5 shows a schematic model of the step height variation, which shows that the average particle size is smaller than the scale of the oxide space (the initial step height of the film is about 350 nm). Therefore, at the beginning of the polishing process (T0), the abrasive particles could be trapped and inactive. The edge corner of the oxide step can be polished preferentially, due to the concentration of the downward acting force. As polishing progresses (T1), the abrasives in the oxide space become active and can support this downward acting force. The probability of direct contact occurring between the oxide layer and the abrasive particles embedded in the pad increases with decreasing step height, and this allows the removal rate of the oxide to increase as planarization progresses. The effect of the abrasive size on the step height variation can be explained in a similar manner. The average size of the abrasive particles in slurry A is the smallest and, therefore, the possibility of them being trapped in the oxide space and thus being inactive during polishing is the greatest. In this case, the oxide removal rate is the lowest and the time to reach the transition to a fast removal rate is the longest. The amount of dishing increases with increasing over-polishing time, as would be expected (Fig. 6). The amount of dishing increases with increasing average abrasive size. The inaction of the abrasives trapped in the oxide space during the initial period of polishing was confirmed by the variation in the roughness (Fig. 7). In the case of slurry A, the surface roughness of the down area after polishing for 20 s remained at about the same level as the roughness of the oxide without polishing. The roughness after polishing decreased with increasing abrasive size. These results confirm that the partial interactions between the abrasive particles and the down area of the oxide decrease with decreasing abrasive size and polishing time, due to the increasing number of trapped and inactive particles. Considering the effect of these inactive particles, the roughness of the down area would be expected to vary significantly with the polishing time. The roughness of the oxide was inversely proportional to the abrasive size but linearly for polishing before the end-point but linearly varied with abrasive size for over-polishing. Variation of roughness with abrasive size after over-polishing matches well with the dishing variation shown in Fig. 6.

4. Conclusion

In this study, the effect of the abrasive size on the step height variation and amount of dishing during STI–CMP was studied. The removal rate of the oxide varied with the polishing time and type of abrasive in the slurry. The unique characteristics of the step height variation associated with the ceria-based slurries were explained by the contribution of the inactive particles, which depended on the height of the remaining oxide layer. The amount of dishing increased as the particle size increased, due to the increasing penetration depth. The roughness of the oxide down area seemed to be well matched with the step height variation and the amount of dishing, which supports the proposed explanation. This study suggests that the size of the abrasive is an important parameter involved in controlling the local planarity in STI–CMP.

Acknowledgements

This work was supported by the Memory Research and Development Division, Hynix Semiconductor Inc.

References

[1] P. Sallagoity, F. Gaillard, M. Rivoire, M. Paoli, M. Haond, Microelectron. Reliab. 38 (1998) 271.
[2] A. Nag, A. Chatterjee, Solid State Technol. 99 (1997) 129.
[3] S.Y. Kim, M.K. Baek, C.I. Kim, E.G. Chang, Electrochem. Soc., Proc. 99 (1999) 2.
[4] T. Izumitani, M. Tomozawa, R. Doremus (Eds.), Treatise on Materials Science and Technology, Academic Press, New York, 1979, p. 115.
[5] S.H. Lee, et al., Jpn. J. Appl. Phys. 37 (1998) 1222.
[6] J.M. Boyd, et al., J. Electrochem. Soc. 143 (1996) 3718.
[7] H.D. Jeong, 15th Korean CMPUGM for New Technology in CMP Processing, 2001.
[8] E. Tseng, et al., VMIC Conference, 1999, p. 270.
[9] T. Mallon, et al., Proceedings of 1997 International CMP for VLIS/ULSI Multilevel Interconnection Conference (CMP-MIC), Santa-Clara, CA, Feb., 173.
[10] B. Zhao, F.G. Shi, Electrochem. Solid-State Lett. 2 (1999) 145.
[11] Ki-Sik Choi, et al., Proc., 4th Inter. CMP-MIC, 1999, p. 307.
[12] H. Nojo, M. Kodera, R. Nakata, Proc. IEEE idem, San Francisco, CA, 1996, p. 349.
[13] Y. Homma, T. Furusawa, K. Kusukawa, M. Nagasawa, Proc. CMP-MIC, Santa Clara, CA, 1996, p. 67.